Influence of Ground Surface Shape and Poisson's Ratio on Three-Dimensional Factors of Safety

Pedro Rogério R. Adriano
Programa de Pós-Graduação em Geotecnia e Construção Civil
Federal University of Goiás, Goiânia, Brasil

José Henrique Fernandes
Escola de Engenharia Civil
Federal University of Goiás, Goiânia, Brasil

Gilson de F. N. Gitirana Jr.,
Programa de Pós-Graduação em Geotecnia e Construção Civil
Federal University of Goiás, Goiânia, Brasil

Murray D. Fredlund
SoilVision Systems Ltd., Saskatoon, Canada

ABSTRACT
This paper presents three-dimensional analyses of hypothetical slopes with simple ground surface shapes. Three-dimensional and two-dimensional factors of safety (FS_{3D} and FS_{2D}, respectively) were compared for several geometry and stress conditions. The ground surface was varied from convex to concave shapes. Poisson's ratio was varied in order to investigate the influence of horizontal stresses. The analyses were performed using formulations recently developed and implemented in the software packages SVOffice 2006 and FlexPDE. The results of this study indicate that the computed FS_{3D} is 26% to 50% higher than FS_{2D}, with larger differences corresponding to concave surfaces. Poisson's ratio influence was clearly demonstrated for three-dimensional conditions. Higher factors of safety were obtained for higher Poisson's ratios.

RÉSUMÉ
Quand des sols contaminés sont chauffés, la pression de vapeur des composés chimiques organiques augmente. L'augmentation de la volatilité aide à l'élimination des contaminants par des méthodes conventionnelles telles l'extraction par vapeur et l'extraction à phases multiples. On peut chauffer le sol par des méthodes électriques in-situ en utilisant le chauffage par conduction conventionnel, le chauffage électrique par résistance ou le chauffage par électromagnétisme.

1 INTRODUCTION

Most slope stability problems present three-dimensional characteristics that are not taken into account by conventional models. Two-dimensional plane strain representations correspond to field condition only in very specific situations. Some of the typical field conditions that are believed to be better represented by full three-dimensional models are excavation fronts, slope corners, and earth dams, to name only a few problems.

Numerous advances in the techniques of geotechnical engineering analysis have emerged in the past two decades, mostly due to the increase in computational power. In fact, one of the potential areas of advance are those areas related to techniques of 3D analysis.

A considerable amount of research has been directed towards the development and improvement of computational tools for three-dimensional analysis. It appears that there is a need to further advance the research, in order to bring this type of analysis into geotechnical engineering practice. It is important that 3D techniques be based on sound theories that are at the same time based on familiar concepts adopted in conventional 2D analysis.

This paper presents a general theory, based on a well known 2D method of slope stability using finite element stress fields. This method is often referred to as "Kulhawy's method" or "enhanced method". Analyses are presented in order to demonstrate the relationship between 3D and 2D factors of safety and the effect of Poisson's ration on this relationship. The influence of ground surface shape is also investigated, in order to illustrate the typical variations to be expected.

2 LITERATURE REVIEW

The methods of three-dimensional analysis of slope stability are usually extensions of conventional two-dimensional approaches. Variational calculus, for instance, has been extended to three-dimensional conditions by Chen and Chameau (1982). The method proposed was an extension of Spencer's method (Spencer, 1967) that is based on the limit equilibrium method of slices. Hungr et al. (1989) presented an extension of Bishop's simplified method (Bishop, 1955), also based on the method of slices. Lam and Fredlund (1993) presented an extension of the GLE limit equilibrium method to three-dimensional conditions. Chang (2002) proposed an extension of Sarma's method (Sarma, 1979). The method is based on blocks that have faces that are not necessarily vertical.

Variational calculus has also been extended to three-dimensional conditions (Leshchinsky et al., 1985 and Leshchinsky and Baker, 1986). Leshchinsky and Huang (1992) further extended their original work, but the method was limited to problems with symmetric geometry.

Michalowski (1989) presented a three-dimensional solution based on the upper-bound theorem. The solution was limited to homogeneous slopes. More recently, Farzaneh and Askari (2003) have extended the work by Michalowski (1989) to non homogeneous slopes. Chen et al. (2001a, 2001b) have also presented an upper-bound solution for three-dimensional slope stability. Lyamin and Sloan (2002a and 2002b) proposed the use of the upper and lower-bound theorems, along with the finite element method, in order to produce stress and strain fields.

From the point of view of practicing geotechnical engineers, it becomes difficult to determine what three-dimensional method of slope stability analysis is the more adequate. A sound theoretical basis, a generalized approach that is capable of handling field conditions, and simplicity, are some of the requirements of a practical slope stability method. It appears that if a practical three-dimensional finite element tool for stress and seepage analysis is available, it becomes convenient to extend the two-dimensional enhanced method to three-dimensional conditions. Such method could be considered a practical tool for routine analyses.

3 THEORY

The analysis method presented herein is an extension of Kulhawy's method (or enhanced method), to three-dimensional conditions. The factor of safety is defined as the ratio by which the shear strength must be reduced in order to bring the soil mass to a state of limit equilibrium. For a three-dimensional slip surface, the factor of safety may be computed by taking the total resisting shear force divided by the total shear force:

$$F_s = R/S = \int_A \tau_f \, dA \Big/ \int_A \tau_a \, dA \tag{1}$$

where: R is the total resisting shear force; S is the total shear force; τ_f is the shear strength; τ_a is the shear stress; and A is the slip surface area.

The resisting and shearing stresses acting along a three dimensional slip surface must be determined. The state of stress and pore-water pressure at any point in the soil volume is determined using the finite element method. The computation of the factor of safety can be summarized as follows:

- The distribution of stresses and pore-water pressures are determined using the finite element method. Appropriate boundary conditions, constitutive models, and constitutive parameters must be adopted;
- The normal and shear stresses are computed for a grid of points located at the base of the slip surface. The normal stress depends on the position along the slip surface. The shear stress depends not only on the position at the slip surface but also on the direction of slippage projected on the horizontal plane;
- Integration of the acting and resisting stresses is performed along the slip surface area.

Spherical and ellipsoidal slip surface shapes have been implemented by Adriano (2008), but only spherical shapes are used herein. The shape and position of a spherical slip surface are defined as follows:

$$z = z_{0s} - \sqrt{r_s^2 - (x - x_{0s})^2 - (y - y_{0s})^2} \tag{2}$$

where: x_{0s}, y_{0s}, and z_{0s} are the coordinates of the center of the sphere in the x, y, and z directions; and r_s is the radius of the slip surface. Only the bottom half of the sphere is taken by using the negative value of the square root.

The direction of a plane tangent to any point on the slip surface is defined by the angles its normal makes with x, y, and z, which is given by the direction cosines:

$$a_{11} = \frac{\partial f / \partial x}{\|f\|} \quad a_{21} = \frac{\partial f / \partial y}{\|f\|} \quad a_{31} = \frac{\partial f / \partial z}{\|f\|} \tag{3}$$

where: *f* denotes the equation defining the geometric location of the slip surface (Eq. 2) and $\|f\| = \sqrt{(\partial f/\partial x)^2 + (\partial f/\partial y)^2 + (\partial f/\partial z)^2}$. The first index indicates the *x*, *y*, and *z* directions. The second index indicates the direction normal to the surface.

For a spherical slip surface, the derivatives are as follows:

$$\begin{aligned} \partial f/\partial x &= 2(x - x_{0s}) \\ \partial f/\partial y &= 2(y - y_{0s}) \\ \partial f/\partial z &= 2(z - z_{0s}) \end{aligned} \tag{4}$$

The normal stress acting in a plane tangent to any point of the slip surface is given by the following equation:

$$\begin{aligned} \sigma_n = {} & \sigma_x a_{11}^2 + \sigma_y a_{21}^2 + \sigma_z a_{31}^2 \\ & + 2\tau_{xy} a_{11} a_{21} + 2\tau_{yz} a_{21} a_{31} + 2\tau_{zx} a_{31} a_{11} \end{aligned} \tag{5}$$

Given the computed σ_n, the shear strength can be calculated using the Mohr-Coulomb criterion for saturated/unsaturated soils:

$$\tau_f = c' + (\sigma_n - u_a)\tan\phi' + (u_a - u_w)\tan\phi^b \tag{6}$$

where: *c*' is the effective cohesion; u_a is the pore-air pressure; ϕ' the angle of internal friction; u_w is the pore-water pressure; and ϕ^b is the angle of friction with respect to changes in matric suction. Equation 6 reduces to the conventional Mohr-Coulomb criterion when the soil becomes saturated.

In order to compute the acting shear stress, the direction of slippage movement must be known. The direction of the slippage movement may be determined as part of the optimization technique used in the determination of the critical slip surface. The slippage direction may also be adopted. For instance, the slippage movement could be assumed to be given by the average slope face direction.

The projection of slippage direction in the horizontal plane is given by a unit vector with components in the *x* and *y* direction, b_1 and b_2. The third component, b_3, indicates the direction normal to the slip surface and is orthogonal to b_1 and b_2:

$$b_3 = (-a_{11} b_1 - a_{21} b_2)/a_{31} \tag{7}$$

The direction cosines that indicate the slippage direction are as follows:

$$\begin{aligned} a_{12} &= b_1 \Big/ \sqrt{b_1^2 + b_2^2 + b_3^2} \\ a_{22} &= b_2 \Big/ \sqrt{b_1^2 + b_2^2 + b_3^2} \\ a_{32} &= b_3 \Big/ \sqrt{b_1^2 + b_2^2 + b_3^2} \end{aligned} \tag{8}$$

Finally, the shear stress acting at any point and slippage direction at the base of the slip surface is given by the stress state and direction cosines, defined by Eqs. 3 and 8:

$$\begin{aligned} \tau_a = {} & \sigma_x a_{11} a_{12} + \sigma_y a_{21} a_{22} + \sigma_z a_{31} a_{32} \\ & + \tau_{xy}(a_{11} a_{22} + a_{21} a_{12}) + \tau_{yz}(a_{21} a_{32} + a_{31} a_{22}) \\ & + \tau_{zx}(a_{31} a_{12} + a_{11} a_{32}) \end{aligned} \tag{9}$$

Finite Element models usually employ procedures based on stresses that are computed at the integration points. Therefore, in order to compute the normal and shear stress at any point at the base of a given slip surface, the state of stress determined at the integration points must be used. If necessary, these stresses can be extrapolated to the nodes using simple mapping techniques. The procedure presented herein must be employed for each trial slip surface established during the optimization analysis. Several optimization techniques are available for critical slip surface search.

4 DESCRIPTION OF HYPOTHETICAL SLOPES ANALYZED

There are few practical tools of numerical analysis capable of analyzing three-dimensional stress states. Most available tools are not practical and efficient, therefore not being adequate for routine geotechnical design.

The analyses presented herein were undertaken using the software package SVOffice 2006 (SoilVision Systems Ltd., 2007). The theory presented in the last section was implemented using FlexPDE (PDE Solution Inc., 2007). FlexPDE is a general-purpose partial differential equation (PDE) solver. FlexPDE is capable of solving 1D, 2D, and 3D PDEs that can be steady-state, transient, linear, or nonlinear. Numerical integration, such as that required by Eq. 1, can be performed for any defined variable. Scripts on a specifically developed language are used in order to develop model in FlexPDE. The formulation presented herein has been verified by Gitirana Jr. et al. (2008) using several benchmark problems.

The hypothetical problems analyzed herein represent a slope with varying shapes, namely concave, plane or convex (Fig. 1). The mid cross-section was maintained at a constant slope of 1V:2H and the slip surfaces analyzed for all scenarios present the same shape and position with respect to the mid-cross section (see Fig 1a). The shape of the ground surface was varied by adopting different values of α (Fig. 1).

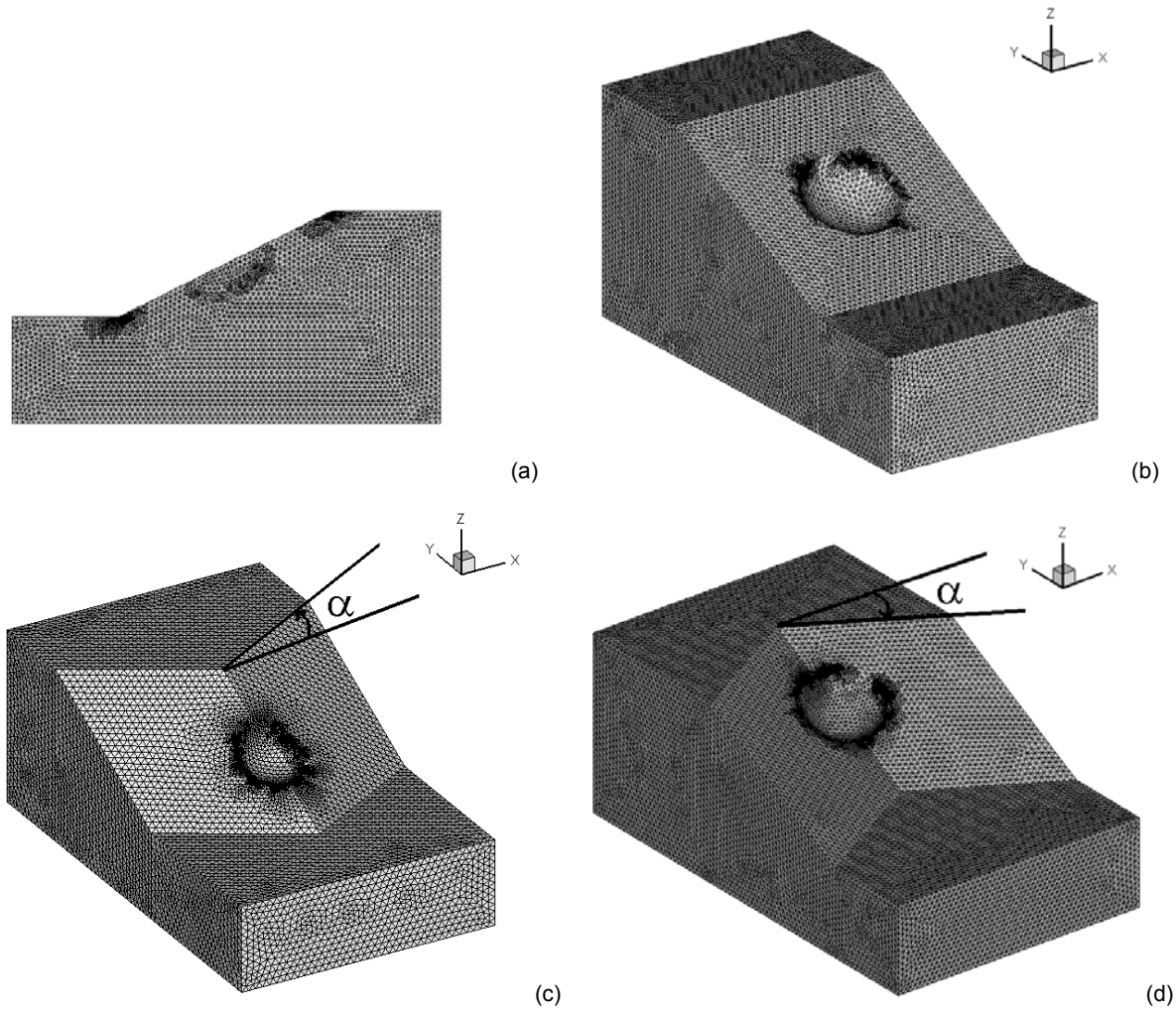

Figure 1. Hypothetical slopes analyzed: (a) two-dimensional slope; (b) Three-dimensional slope with plane shape; (c) Three-dimensional slope with convex shape; d) Three-dimensional slope with concave shape.

The hypothetical parameters adopted herein for the linear elastic analysis of stresses using finite elements are as follows: Young Modulus of 3500 kPa, Poisson's coefficient varying from 0.1 to 0.49 and unit weight of 1 kN/m^3. The shear strength parameters adopted correspond to a cohesive material with cohesion of 0.1 kPa. Pore-water pressure effects are not taken into account. This combination of parameters and geometry of the mid-section is identical to that studied by Hungr et al. (1989). Chen at al. (2001a) has analyzed the same slope, with a different but equivalent combination of shear strength and unit weight values.

The critical slip surface adopted has a radius of 1 m and its center is located at coordinates x = 2, y = 1.78 and z = 1.45. Boundary conditions were established in order to allow the generation of stresses due to the self-weight of the soil without boundary effects. The lower boundary was subjected to an essential boundary condition representing zero displacements. The lateral boundaries suffered restriction on the x-displacements (see Fig. 4 for an indication of the x- y- and z- directions with respect to the problem domain). The front and back boundaries was fixed in the y direction. The ground surface was let free to move and no external load was applied.

5 RESULTS AND DISCUSSION

This section presents the result of analyzes of hypothetical slopes and the discussion of the results.

5.1 5.1 Analysis of the Sensitivity of the Factor of Safety to Mesh Control Parameters

FlexPDE adopts a number of mesh control parameters that can be employed in a variety of ways, in order to obtain accuracy levels required. The parameter "Errlim" determines the amount of automatic mesh refinement that will take place during an analysis. "Errlim" is an important parameter during stress analyses. The parameter "NGRID" controls the mesh density at the beginning of an analysis and is a convenient control parameter for stress integration along a given slip surface. It is important to point out that stress integration is performed in a separate numerical model, taking the stress field previously computed along with the slip surface shape and position adopted.

The slope geometry presented in Fig. 1b was analyzed with varying valued of "Errlim" and "NGRID", in order to

establish appropriate values. The computed factor of safety and the computation time were adopted as reference parameters to be evaluated.

Figure 2 presents the results obtained by varying "Errlim". Relatively low factors of safety are obtained for coarse meshes obtained using Errlim = 1×10^{-1} to 1×10^{-2}. A "well behaved" trend is observed for lower values of "Errlim" and the factor of safety appears to the insensitive when "Errlim" is equal of lower than 1×10^{-5}. A value of 1×10^{-4} appears to provide sufficiently accurate results at a considerably lower computational cost.

Figure 3 presents the results obtained by varying "NGRID". The factors of safety appear to increase when using finer meshes (i.e., larger values of "NGRID"). The changes in factor of safety appear to reduce to insignificant values for NGRID beyond 40 or 50. However, the computation time when using NGRID of 50 is considerably higher. Therefore, a value of NGRID = 40 appears to provide a better balance between accuracy and analysis time.

In summary, based on these analyses it is recommended that a value of "Errlim" of 1×10^{-4} and a value of "NGRID" of 40 be adopted. These values have been employed in all further analyses presented herein, except for a few cases, which will be discussed later.

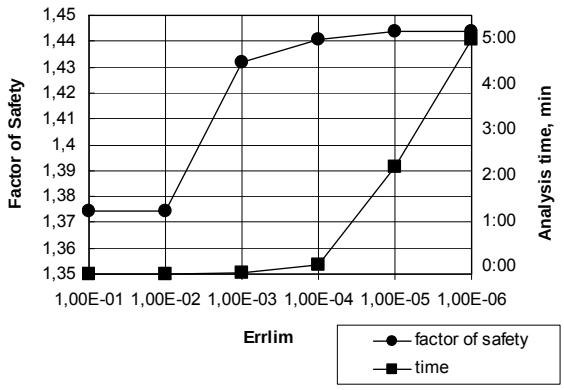

Figure 2. "Errlim" versus the factor of safety and the analysis time.

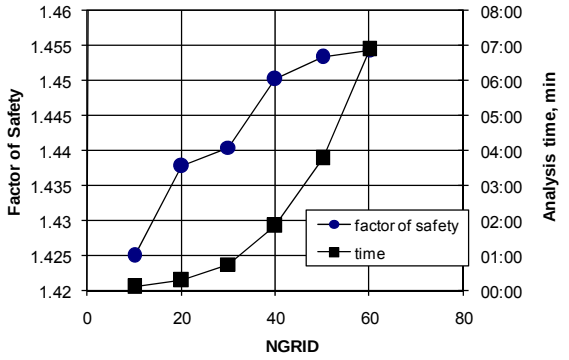

Figure 3. "NGRID"versus the factor of safety and the analysis time.

It is also important to point out that the computation times can be kept within acceptable limits while guaranteeing an accurate numerical solution. This is an important departure from last decade's 3D numerical models, which could not be used in routine due to unacceptable computational requirements.

5.2 5.2 Analysis 3D Factors of Safety for Varying Geometries and Stress Conditions

The two-dimensional factor of safety obtained for the 2D cross section presented in Fig 1a was 1.085. This value serves as a basis of comparison for all remaining analysis, which will all be three-dimensional. This cross section is identical to the mid cross section of all 3D geometries analyzed herein. Therefore, the FS_{2D} obtained for that cross section can be interpreted as the factor of safety that would be obtained by a geotechnical engineer employing conventional 2D tools and selecting the "most representative" cross section.

Figure 4 presents a typical plot of vertical stresses obtained when solving the PDEs governing the equilibrium of forces. Similar plots are also obtained for the remaining stress state components. After quick inspection of Fig. 4 it can be seen that the vertical stresses are compatible what would be expected based on the unit weight adopted for the material.

Figure 5 summarizes the results obtained herein for the various geometries and Poisson's ratio values. It can be observed that the factors of safety increase as the surface geometry moves from convex towards concave conditions. This result was expected based on the arch effect widely reported in the literature.

It is also interesting to note that all the 3D factors of safety obtained are higher than the 2D factor of safety obtained at the mid cross section (FS_{2D} = 1.085). The lowest value of FS_{3D} obtained was approximately 26% higher than the value of FS_{2D}. This difference is due to the border effects that are taken into account on a 3D analysis and completely disregarded on the conventional 2D analysis.

Moving towards concave conditions, the arch effect start to cause and increase on the FS_{3D}, which, combined with the border effects, will cause an increase of the FS_{3D}/FS_{2D} ratio in the order of 50%.

Poisson's ratio appears to have a significant effect on the values of FS_{3D}. Larger values of Poisson's ratio appear to result in an increase in the factor of safety. This is due to the decrease in deviator stresses generated by the self-weight of the soil. One interesting effect of Poisson's ratio was the change in the variation of FS_{3D} for concave geometries. Larger values of Poisson's ratio have resulted in values FS_{3D} that are not dependent on the angle defining the concave geometry. As the values of Poisson's ratio decrease, the angle of the concave surface starts to affect the value of FS_{3D}.

Fig. 6 presents plots illustrating the distribution of local factors of safety for four selected geometries. The results obtained are as expected, with higher values along the crest and foot of the slopes. The comparison between 2D and 3D representations helps understanding the arch effect.

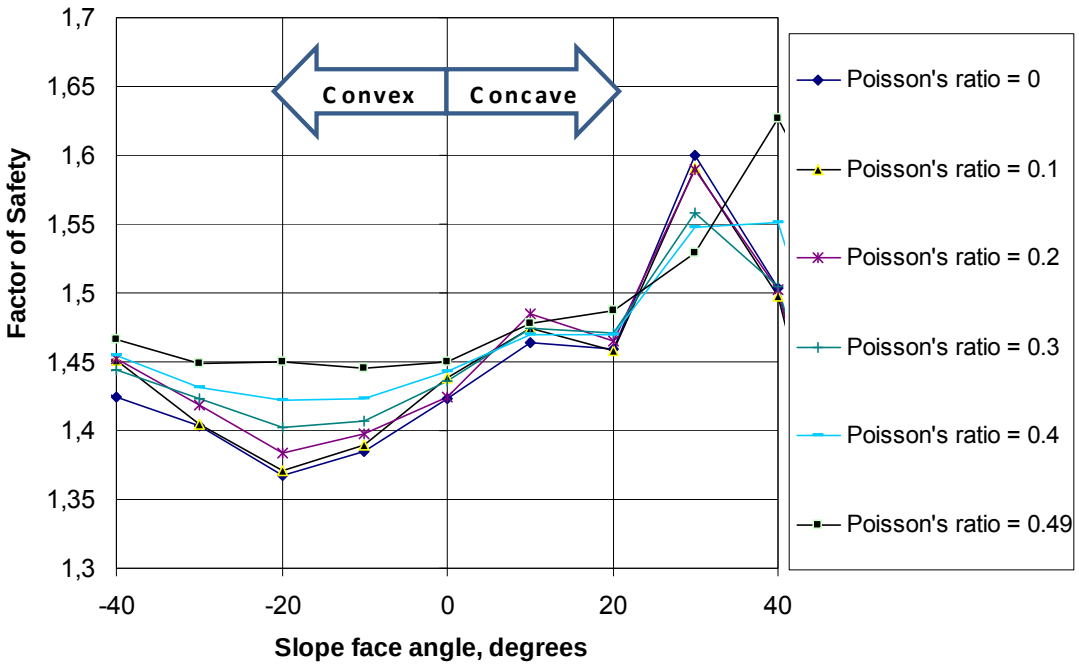

Figure 5. Three-dimensional factor of safety for various scenarious.

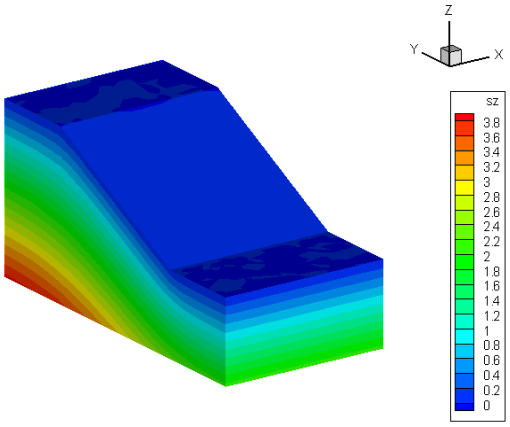

Figure 4. Vertical stress istribution.

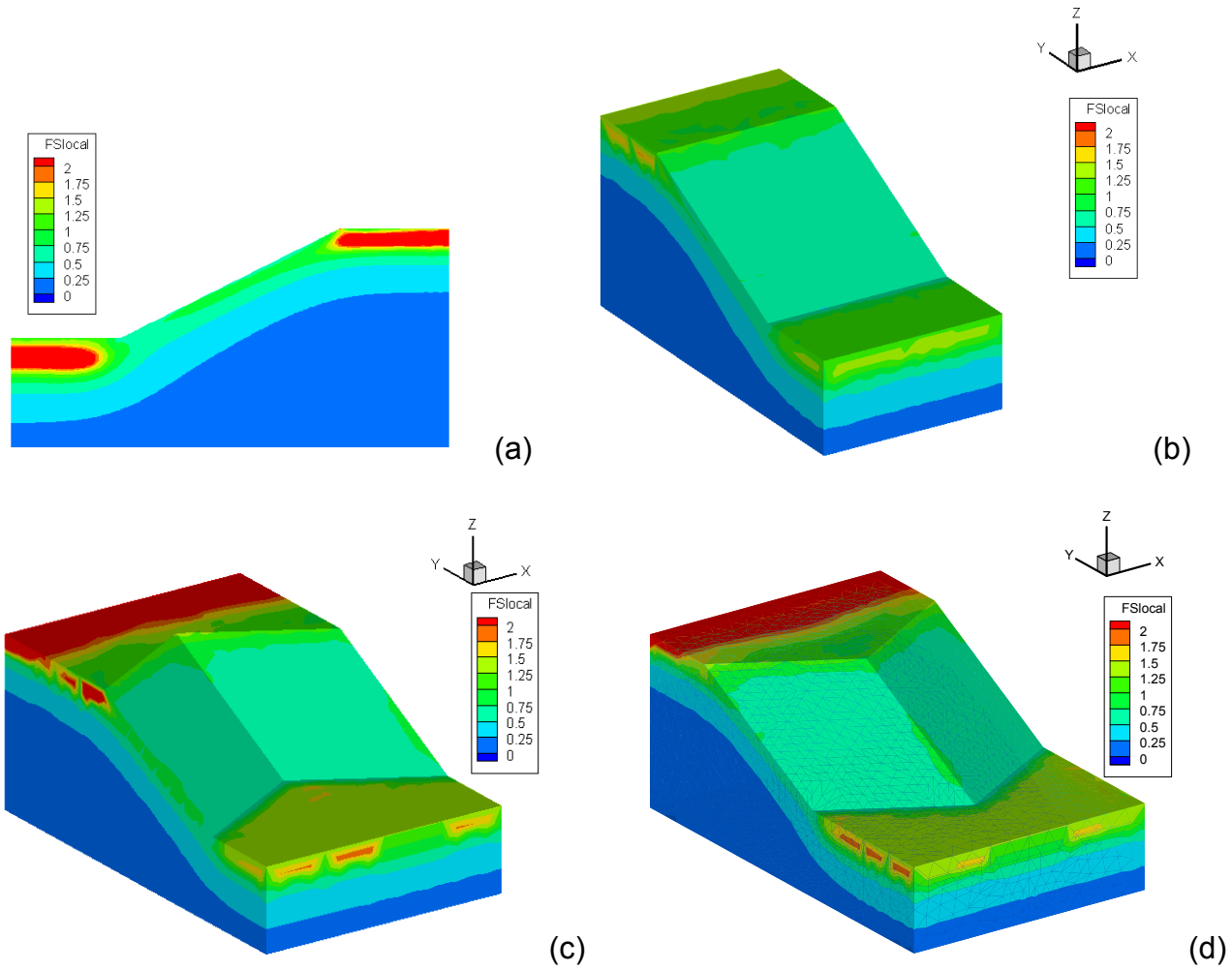

Figure 6. Local factor of safety for Poisson's ratio of 0.3: a) Two-dimensional analysis; (b) Three-dimensional slope with plane shape; (c) Three-dimensional slope with convex shape; d) Three-dimensional slope with concave shape.

Figure 6c clearly indicated the arch effect, which is absent in the remaining figures. This effect is apparent by the contours of higher factor of safety that move towards the mid cross section of the domain.

6 CONCLUSIONS

This paper presented a methodology for computing three-dimensional factors of safety. The method has been implemented and tested for various conditions. The results indicate that the computational cost is reasonable, with typical analyses taking less than 10 minutes for completion. Model setup times are also kept low thanks to a user-friendly interface and to the fact that the finite element mesh is automatically generated.

Several slope surface geometries were analyzed and the results compared to the two-dimensional factor of safety. Poisson's ratio was also varied during the analyses. The differences between two- and three-dimensional factors of safety are significant and indicate that FS_{3D} can often be excessively conservative. The ratio between FS_{3D} and FS_{2D} varied from 26% to 50%, depending on the ground surface shape. Poisson's ratio also plays a significant role on the 3D factors of safety.

ACKNOWLEDGEMENTS

This research project received financial and/or in-kind support from CAPES, CNPq and SoilVision Systems Ltd.

REFERENCES

Adriano, P.R.R. (2008). Two- and Three-dimensional analysis of slope stability using the enhanced method. Master's Thesis. Programa de Pós-Graduação em Geotecnia e Construção Civil, UFG. (in preparation).

Bishop, A. W. (1955). The use of the slipe circle in the stability analysis of slopes. Géotechnique 5, No. 1, 7-17.

Chang, M. (2002). A 3D slope stability method assuming parallel lines of intersection and differential straining of blocks contacts. Can. Geotech. J. 39. 799-811.

Chen, R. H.; Chameau, J. L. (1982). Three-dimensional limit equilibrium analysis of slopes. Géotechnique 32. 31-40.

Chen, Z. Y., Wang, X. G., Haberfield, C., Yin, J. H. and Wang, Y. J. (2001a). A three-dimensional slope stability analysis method using the upper bound theorem. Part I: Theory and methods. Int. J. Rock Mech. Mining Sci. 38: 369–378.

Chen, Z. Y., Wang, J., Wang, Y. J., Yin, J. H. and Haberfield, C. (2001b). A three-dimensional slope stability analysis method using the upper bound theorem. Part II: Numerical approaches, applications and extensions. Int. J. Rock Mech. Mining Sci. 38: 379-397.

Farzaneh, O. & Askari, F. (2003). Three-dimensional analysis of nonhomogeneous slopes. J. Geotech. Geoenviron. Engng ASCE, 129(2): 137-145.

Gitirana Jr., G. F. N., Santos, M. A. A., Fredlund, Murray D. (2008). Tree-dimensional slope stability model using finite element stress analysis. GeoCongress, New Orleans. 1-8.

Hungr, O., Salgado, F.M. and Byrne, P.M. (1989). Evaluation of a three-Dimensional Method of Slope stability analysis. Can. Geotech. J. 26: 679-686.

Lam, L. and Fredlund, D.G (1993). A general limit equilibrium model for three-dimensional slope stability analysis, Can. Geotech. J. 30: 905-919.

Leshchinsky, D., Baker, R. and Silver, M. L. (1985). Three dimensional analysis of slope stability. Int. J. Numer. Anal. Methods Geomech., 9: 199–223.

Leshchinsky, D. and Baker, R. (1986). Three-dimensional slope stability: end effects. Soil and Foundations, 26 (4): 98-110.

Leshchinsky, D. and Huang, C. C. (1992). Generalized three-dimensional slope stability analysis. J. Geotech. Engng ASCE 118 (11): 1748–1764.

Lyamin, A. V. & Sloan, S. W. (2002a). Lower bound limit analysis using nonlinear programming. Int. J. Numer. Methods Engng, 55 (5): 573–611.

Lyamin, A. V. & Sloan, S. W. (2002b). Upper bound limit analysis using linear finite elements and non-linear programming. Int. J. Numer. Anal. Methods Geomech., 26: 181-216.

Michalowski, R. L. (1989). Three-dimensional analysis of locally loaded slopes. Geotechnique, 39 (1): 27–38.

PDE Solutions Inc. (2007). FlexPDE 5.0 - Reference Manual, Antioch, CA, USA.

Sarma, S. K., (1979). Stability analysis of embankments and slopes. Journal of the Geotechnical Engeneering Division, ASCE, 105(GT 10): 1511-1524.

SoilVision Systems Ltd. (2007). “SVOffice 2006 User’s and Theory Guide.” Saskatoon, SK, Canada.

Spencer, E. (1967). A method of analisys of the stability of embankments assuming parallel interslica forces. Géotechnique 17, No. 1, 11-26.